

1 **GIGANTEA recruits deubiquitylases, UBP12 and UBP13, to regulate**
2 **accumulation of the ZTL photoreceptor complex**

3

4 Chin-Mei Lee, Man-Wah Li, Ann Feke, Adam M. Saffer, Wei Liu, Joshua M. Gendron

5

6 Department of Molecular, Cellular and Developmental Biology, Yale University, New Haven,

7 CT, USA, 06511

8 **Abstract**

9 To remain synchronous with the environment, plants constantly survey daily light conditions
10 using an array of photoreceptors and adjust their circadian rhythms accordingly. ZEITLUPE
11 (ZTL), a blue light photoreceptor with E3 ubiquitin ligase activity, communicates end-of-day
12 light conditions to the circadian clock. To function properly, ZTL protein must accumulate but
13 not destabilize target clock transcription factors before dusk, while in the dark ZTL mediates
14 degradation of target proteins. It is not clear how ZTL can accumulate to high levels in the light
15 while its targets remain stable. Two deubiquitylating enzymes, UBIQUITIN-SPECIFIC
16 PROTEASE 12 and UBIQUITIN-SPECIFIC PROTEASE 13 (UBP12 and UB13), which have
17 opposite genetic and biochemical functions to ZTL, were shown to associate with the ZTL
18 protein complex. Here we demonstrate that the ZTL light-dependent interacting partner,
19 GIGANTEA (GI), recruits UB12 and UB13 to the ZTL photoreceptor complex. We show that
20 loss of *UB12* and *UB13* reduces ZTL and GI protein levels through a post-transcriptional
21 mechanism. Furthermore, the ZTL target protein TOC1 is unable to accumulate to normal levels
22 in *ubp* mutants, indicating that UB12 and UB13 are necessary to stabilize clock transcription
23 factors during the day. Our results demonstrate that the ZTL photoreceptor complex contains
24 both ubiquitin-conjugating and -deconjugating enzymes, and that these two opposing enzyme
25 types are necessary for the complex to properly regulate the circadian clock. This work also
26 shows that deubiquitylating enzymes are a core design element of circadian clocks that is
27 conserved from plants to animals.

28

29 **Main**

30 Circadian clocks in all organisms rely on photoreceptors to sense light and entrain the central
31 oscillator. The exact timing of the light-to-dark transition (dusk) is especially important for
32 plants, as this indicates the length of the day and provides seasonal timing information necessary
33 for the adjustment of plant developmental processes (Carre, 2001; Yanovsky and Kay, 2002;
34 Imaizumi et al., 2003; Salome and McClung, 2004; Imaizumi and Kay, 2006; Nozue et al., 2007;
35 Mizoguchi and Yoshida, 2009; Ito et al., 2012). One way that plants sense the end of the day is
36 by using a unique photoreceptor called ZEITLUPE (ZTL) to control the stability of circadian
37 clock transcription factors differentially in the light and the dark (Somers et al., 2000). ZTL
38 contains an N-terminal light-oxygen-voltage sensing (LOV) domain which senses blue light.
39 Adjacent to the LOV domain are the F-box domain, which allows ZTL to function as an E3
40 ubiquitin ligase, and a Kelch-repeat domain. ZTL mediates degradation of transcription factors
41 that are at the core of the plant circadian clock including TIMING OF CAB2 EXPRESSION 1,
42 PSEUDO-RESPONSE REGULATOR 5, and CCA1 HIKING EXPEDITION (TOC1, PRR5, and
43 CHE) (Mas et al., 2003; Han et al., 2004; Kiba et al., 2007; Fujiwara et al., 2008; Baudry et al.,
44 2010; Lee et al., 2018). In the light, ZTL accumulates to high levels but is unable to mediate
45 degradation of the clock transcription factors (Kim et al., 2003; Kim et al., 2007). The
46 accumulation of ZTL protein during the day is dependent on interaction with the co-chaperone
47 protein GIGANTEA (GI) (Kim et al., 2013; Cha et al., 2017; Cha et al., 2017). GI interacts with
48 ZTL through the LOV domain in the light and dissociates from ZTL in the dark, allowing ZTL to
49 mediate degradation of its target proteins and then be degraded by the ubiquitin proteasome
50 system, likely through autocatalytic activity (Kim et al., 2003; Mas et al., 2003; Somers et al.,
51 2004; Kiba et al., 2007; Kim et al., 2007; Kim et al., 2011; Kim et al., 2013). One of the roles of

52 GI is to recruit HSP70/HSP90 for maturation of the ZTL protein in the light, but ZTL is unable
53 to mediate ubiquitylation and degradation of target proteins until dark (Mas et al., 2003; Kiba et
54 al., 2007; Fujiwara et al., 2008; Cha et al., 2017; Pudasaini et al., 2017). It was proposed that GI
55 can promote maturation of ZTL and block or counteract ZTL activity; however, this second role
56 for GI has not been investigated in depth (Fujiwara et al., 2008; Pudasaini et al., 2017).

57
58 We previously identified ZTL-interacting proteins using immunoprecipitation followed by mass
59 spectrometry (IP-MS) with a “decoy” ZTL that lacks E3 ubiquitin ligase activity and stably binds
60 interacting proteins (Lee et al., 2018). We identified UBIQUITIN-SPECIFIC PROTEASE 12
61 and 13 (UBP12 and UB13) as high confidence ZTL-interacting proteins which were shown
62 previously to have an unspecified role in clock function (Cui et al., 2013; Lee et al., 2018).

63 UB12 and UB13 also interact with GI in IP-MS experiments (Krahmer et al., 2019),
64 suggesting that either the UBPs interact with ZTL and GI independently or that ZTL, GI, and the
65 UBPs exist together in a complex. UB12 and UB13 are closely related deubiquitylating
66 enzymes that can cleave lysine 48-linked mono- or poly-ubiquitin from substrates (Ewan et al.,
67 2011; Cui et al., 2013), interestingly, a biochemical role opposite to that of ZTL. In addition to
68 regulating the circadian clock, they are also involved in flowering time, pathogen defense, root
69 differentiation, and hormone signaling (Ewan et al., 2011; Derkacheva et al., 2016; Jeong et al.,
70 2017; Zhou et al., 2017; An et al., 2018). We performed yeast two-hybrid assays and found that
71 UB12 and UB13 interacted with GI but not with ZTL or the ZTL target proteins TOC1,
72 PRR5, or CHE (Fig.1a). We next tested the interaction between GI and UB12 and UB13 *in*
73 *planta* via bimolecular fluorescence complementation (BiFC) in *Arabidopsis* protoplasts
74 (Fig.1b). GI, UB12, and UB13 are localized in the cytoplasm and nucleus (Cui et al., 2013;

75 Kim et al., 2013), and our BiFC results show that UBP12 and UBP13 interact with GI in both
76 compartments with strong signal in the nucleus and weaker but detectable signal in the
77 cytoplasm. The interacting complexes of UBP12 and GI formed nuclear foci, similar to the
78 localization of GI alone (Kim et al., 2013). UBP12 and UBP13 contain a MATH-type (meprin
79 and TRAF homology) protein interaction domain and a ubiquitin-specific protease (USP)
80 domain (Fig. S1). The MATH domains of UBP12 and UBP13 were necessary for interaction
81 with GI while the protease domain and the C-terminal portions did not mediate GI-interaction
82 (Fig. 1c). This suggests that the interaction between GI and UBP12 or UBP13 is not dependent
83 on the UBP USP domains binding to poly-ubiquitylated GI protein.

84
85 We next determined whether GI was necessary to bridge the interaction between UBP12 or
86 UBP13 and ZTL *in vivo* by performing IP-MS on wild type (Col-0) and *gi-2* mutant transgenic
87 lines expressing the decoy ZTL protein (Fig. S2). We collected samples at 9 hours after dawn
88 from plants grown in 12h light/12h dark cycles to capture the time when ZTL and GI are
89 normally interacting. We found that UBP12 and UBP13 were enriched in the Col-0 samples (*p*-
90 value= 3.58E-5 and 0.0113 for UBP12 and UBP13 respectively), but not in the *gi-2* mutant (*p*-
91 value= 1 for both) (Fig.1d and Table S1). These results indicate that GI is required for
92 UBP12/UBP13 to form a complex with ZTL, substantiating our interaction studies in
93 heterologous systems. Notably, LKP2, a known ZTL interacting partner, associated with ZTL in
94 the presence or absence of GI and suggests that the decoy ZTL is able to form biologically
95 relevant protein complexes even in the *gi-2* mutant (Takase et al., 2011). Together these results
96 suggest that the GI protein physically bridges the interaction between UBP12 or UBP13 and ZTL
97 *in vivo*.

98

99 As a complementary approach to the IP-MS (Fig.1d) we co-expressed FLAG-UBP12 or FLAG-
100 UBP13 with HA-GI and Myc-ZTL in *N. benthamiana* leaves. We then performed
101 immunoprecipitation with anti-FLAG antibody and detected the presence of FLAG-UBP12,
102 FLAG-UBP13, HA-GI, and Myc-ZTL using western blotting (Fig.1e). In the FLAG
103 immunoprecipitation samples, HA-GI was always detected when co-expressed with FLAG-
104 UBP12 or FLAG-UBP13, showing that UBP12 and UBP13 interact with GI independently of the
105 presence of Myc-ZTL. Furthermore, Myc-ZTL was undetectable in the FLAG
106 immunoprecipitation samples unless co-expressed with HA-GI showing that the interaction
107 between UBP12 or UBP13 and ZTL is dependent on GI. These assays support our previous
108 results (Fig.1a-d) and show that a trimeric complex between full-length ZTL, GI, and UBP12 or
109 UBP13 can form *in vivo* (Fig.1f).

110

111 Our physical interaction model (Fig. 1f) led us to hypothesize that *UBP12* and *UBP13* regulate
112 the circadian clock through the same genetic pathway as *ZTL* and *GI*. We tested this via epistasis
113 analyses with loss-of-function mutants in *ZTL*, *GI*, *UBP12*, and *UBP13*. Previously, it was
114 shown that knockdown of *UBP12* and *UBP13* results in shortened clock periods (Cui et al.,
115 2013). We first determined the period of a series of mutant alleles in *UBP12* and *UBP13* by
116 crossing them to the *pCCA1::LUC* clock reporter transgenic line and measuring luciferase
117 activity (Fig. 2a-d). We found that single mutations in either *UBP12* or *UBP13* shortened the
118 clock period with period lengths that varied from 0.4 to 1 hour shorter than wild type. We next
119 generated *ubp12-1/gi-2* and *ubp13-1/gi-2* double mutants and measured the expression of the
120 core clock gene *CCA1* during a 2-day circadian time course in constant light using qRT-PCR

121 (Fig. 2e-f and Table S2). LS Periodogram analysis using the Biodare2 platform
122 [biodare2.ed.ac.uk (Zielinski et al., 2014)] showed that the *ubp12-1/gi-2* double mutant had a
123 similar phase and amplitude of *CCA1* expression to the *gi-2* mutant alone and a period more
124 similar to *ubp12-1* (Table S3). These results show a non-additive interaction and suggest they
125 function in the same circadian genetic pathway. The *ubp13-1/gi-2* double mutant had a similar
126 amplitude to the *gi-2* mutant but had a more similar phase and period to the *ubp13-1* mutant
127 (Table S3). This again shows a non-additive genetic interaction but also suggests that the roles of
128 *UBP12* and *UBP13* have slightly diverged with respect to clock function. We also crossed the *gi-*
129 *2* mutant with the *ubp12-2w* mutant which had reduced expression of both *UBP12* and *UBP13*
130 and the shortest clock period of the tested *ubp* mutant alleles (Fig.S3, 2a-d). The pattern of *CCA1*
131 expression in the *ubp12-2w/gi-2* double mutant was nearly identical to the *gi-2* mutant, further
132 confirming that the effects of the *UBPs* and *GI* are not additive (Table S3). These results indicate
133 that *UBP12* and *UBP13* work in the same pathway as *GI* to control clock function.
134
135 *ZTL* functions downstream of *GI* to regulate the circadian clock (Kim et al., 2007). Thus, we
136 hypothesized that *ZTL* would function downstream of *UBP12* and *UBP13* as well. To test the
137 genetic interaction between *UBP12* or *UBP13* and *ZTL*, we crossed *ubp12-1* and *ubp13-1* to the
138 *ztl-4* null mutant (Fig. 2g and h). The daily expression patterns of *CCA1* in the *ubp12-1/ztl-4* and
139 *ubp13-1/ztl-4* double mutants were nearly identical to the *ztl-4* mutant alone in phase and
140 amplitude (Table S3). Interestingly, the period data showed that the *ubp12-1/ztl-4* was more
141 similar to *ztl-4* than *ubp12-1*, but the *ubp13-1/ztl-4* is more similar to *ubp13-1*. This data suggests
142 that *ZTL* is epistatic to *UBP12* and *UBP13* but that *UBP13* has diverged in function from
143 *UBP12*. It is important to note that the qRT-PCR data is below the suggested resolution for

144 Biodare2 analysis which can result in inaccurate period calls (i.e. *ubp13-1* period is estimated by
145 Biodare2 as the same period as wild type in this experiment). These results corroborate our
146 physical interaction studies and suggest that *UBP12* and *UBP13* regulate the circadian clock
147 upstream of *ZTL*.

148
149 *UBP12* and *UBP13* are functional deubiquitylases that can cleave poly-ubiquitin from generic
150 substrates (Ewan et al., 2011; Cui et al., 2013). We tested whether this deubiquitylation activity
151 is necessary for their role in circadian clock function. To do this we performed complementation
152 studies with wild-type *UBP12* and mutant *UBP12^{C208S}*. *UBP12^{C208S}* has a mutation in the
153 cysteine-box of the USP enzymatic core (Fig. S1) that renders it non-functional as a
154 deubiquitylase (Cui et al., 2013; Derkacheva et al., 2016; Jeong et al., 2017). We transformed
155 *UBP12-YFP* or *UBP12^{C208S}-YFP* driven by the *UBP12* native promoter into the *ubp12-1* mutant
156 and analyzed a population of T1 transgenic lines. In this experiment we consider a line to have
157 rescued the *ubp12-1* mutant clock phenotype if it has a period length longer than the average
158 period length of the *ubp12-1* plus one standard deviation. Using this criteria, 10 of 32 transgenic
159 lines (31%) transformed with catalytically active *UBP12* rescued the short period defect of the
160 *ubp12-1* mutant. Strikingly, only one transgenic line transformed with the inactive *UBP12^{C208S}*
161 was able to rescue the short period phenotype of *ubp12-1* (Fig. 2i-j). As reference, approximately
162 13% of the *ubp12-1* plants themselves and 62% of the wild type plants fell into the rescue
163 category. This is likely due to normal variations in population level data of this type. We further
164 confirmed that *UBP12-YFP* and *UBP12^{C208S}-YFP* were both localized to the cytoplasm and
165 nucleus, suggesting that differences in the clock phenotypes are not due to mislocalization of the

166 UBP12^{C208S} protein (Fig S4). These results indicate that the deubiquitylating functions of UBP12
167 are necessary for its role in regulating the circadian clock.

168

169 By cleaving poly-ubiquitin from proteins, deubiquitylase enzymes can regulate protein stability
170 and accumulation (Komander et al., 2009; Jeong et al., 2017; Mevissen and Komander, 2017; An
171 et al., 2018). The physical and genetic interactions shown for UBP12, UBP13, GI and ZTL
172 prompted us to hypothesize that the UBP12 and UBP13 regulate GI or ZTL protein levels,
173 allowing for accumulation of the proteins in the end of the day. We measured the level of HA-
174 tagged GI under the control of the GI native promoter (*pGI::GI-HA*) in the *ubp12-1* and *ubp13-1*
175 mutants during a 12h light/12h dark time course (Fig. 3a). GI protein levels were approximately
176 50% lower in the *ubp12-1* and *ubp13-1*. mRNA expression of *GI-HA* was also approximately
177 25% lower than wild type at the peak of *GI* mRNA expression, ZT8 (Fig. 3b). This suggests that
178 GI protein accumulation is partially dependent on UBP12 and UBP13, but that altered
179 transcription of *GI* could also have an effect on GI protein.

180

181 Next, we measured ZTL protein levels in the *ubp12-1* and *ubp13-1* mutants (Fig. 3c). ZTL
182 protein levels were substantially decreased in the *ubp12-1* and *ubp13-1* mutants throughout the
183 entire day/night cycle. Overexposure of the immunoblot showed that a small amount of ZTL
184 protein can still accumulate in the *ubp* mutants (Fig. 3c). The expression of *ZTL* mRNA was
185 largely unaffected in these lines (Fig. 3d), suggesting that the decrease in *ZTL* protein levels was
186 caused by a post-transcriptional mechanism. This is similar to the post-transcriptional control of
187 *ZTL* reported in *gi* loss-of-function mutants (Kim et al., 2007), and indicates that UBP12 and
188 UBP13 are necessary for robust accumulation of the *ZTL* protein.

189
190 Interestingly, the *ubp12-1* and *ubp13-1* mutants caused severe reduction in the levels of the ZTL
191 protein but had a short period phenotype, opposite to the long period phenotype of *ztl* loss-of-
192 function mutants. Normally, loss of ZTL causes aberrantly high levels of TOC1 protein while
193 overexpression of ZTL causes low levels of TOC1 protein (Mas et al., 2003; Kiba et al., 2007;
194 Pudasaini and Zoltowski, 2013; Pudasaini et al., 2017). To determine if UBP12 and UBP13
195 affect TOC1 protein levels, we crossed a transgenic line expressing TOC1 fused to YFP under
196 the *TOC1* promoter (*TMG*) to the *ubp12-1* and *ubp13-1* mutants and measured TOC1 protein
197 levels (Fig. 3e). TOC1 protein levels were severely reduced in the *ubp12-1* and *ubp13-1* mutants
198 while mRNA expression of the *TOC1-YFP* transgene was similar in the wild type and mutant
199 backgrounds, suggesting that the decrease in TOC1 protein levels was caused by a post-
200 transcriptional mechanism (Fig. 3f). Notably, TOC1 protein was unable to accumulate to high
201 levels in the light in the *ubp* mutants (Fig. 3e at 12 hours after dawn). This is similar to the
202 effects of the *gi-2* mutant, where TOC1 protein levels never accumulate to full wild-type levels
203 (Kim et al., 2007). Lowered levels of the TOC1 protein result in shortened period, suggesting
204 this was the cause of the short period phenotype of the *ubp12* and *ubp13* mutants.

205
206 We have shown that UBP12 and UBP13 are components of the ZTL-GI photoreceptor complex
207 that are necessary for accumulation of the proteins in the end of the day. UBP12 and UBP13 can
208 remove poly-ubiquitin from targets non-specifically (Ewan et al., 2011; Cui et al., 2013). Thus,
209 we hypothesize that UBP enzymes are recruited by GI to the ZTL photoreceptor complex to
210 prevent formation of poly-ubiquitin chains, resulting in increased stability of the protein complex
211 (Fig. S5). Interestingly, ZTL protein levels were severely damped in the *ubp12* and *ubp13*

212 mutants, but counterintuitively the ZTL target, TOC1, also had reduced levels (Fig. 3c-f). This
213 effect is similar to what was observed in a *gi* loss-of-function mutant, and suggests that GI and
214 UBP12 and UBP13 can counterbalance the activity of ZTL during the day, allowing TOC1 to
215 accumulate to high levels before being degraded (Kim et al., 2007). Although ZTL levels were
216 decreased in the *ubp* mutants, there was still a small amount that could potentially decrease
217 TOC1 levels in the light (Fig. 3c long exposure). This is different than what was seen when
218 HSP90 activity was inhibited, resulting in lower ZTL levels but higher TOC1 levels. This
219 suggests that HSP90 is necessary for ZTL protein maturation and to promote its activity (Kim et
220 al., 2011). This data in combination with our results suggest that GI performs two roles in the
221 ZTL photoreceptor complex: (1) acting as a co-chaperone that recruits HSP proteins to facilitate
222 ZTL maturation (Cha et al., 2017; Cha et al., 2017), and (2) counterbalancing ZTL's role in
223 ubiquitin conjugation with UBP12 and UBP13 present to deconjugate ubiquitin. The light-
224 regulated nature of the ZTL-GI interaction also indicates that light is controlling the balance of
225 ubiquitin conjugation and deconjugation that allows the ZTL photoreceptor complex to
226 accurately degrade proteins at the correct time of day. It was previously shown that mammalian
227 and insect circadian clocks utilize deubiquitylation to regulate stability and subcellular
228 localization of clock proteins (Scoma et al., 2011; Luo et al., 2012; Yang et al., 2012). In light of
229 this, our results further demonstrate that deubiquitylation activity is an evolutionarily conserved
230 architectural design feature of the clocks of higher eukaryotes Furthermore, the mammalian
231 orthologue of UBP12 and UBP13, USP7, impacts clock function in response to environmental
232 stress (Papp et al., 2015; Hirano et al., 2016) suggesting that these deubiquitylases are conserved
233 clock regulators across evolution.
234

235

236 **Materials and Methods**

237 See supplemental information

238

239 **End notes:**

240 **Acknowledgement**

241 We thank Dr. David E. Somers for providing the anti-ZTL antibody. We would like to thank Dr.

242 Nicole Clay and Dr. Jimi Miller for kindly sharing pABind vectors and the assistance with

243 transient expression in the *Nicotiana benthamiana* experiments, the Keck Proteomics Facility at

244 Yale for processing samples and analyzing proteomic data, Dr. Shirin Bahmanyar, Dr. Marshall

245 Delise and Dr. Joseph Wolenski for assistance with confocal microscopy experiments. Also,

246 Suyuna Eng Ren, Chris Adamchek, Chris Bolick, Christine Ventura, Denise George, and Sandra

247 Pariseau for technical and administrative support. We would like to thank Dr. Vivian Irish, Dr.

248 Mark Hochstrasser and Dr. Eric Bennet for helpful comments on experimentation and the

249 manuscript. This work was supported by NSF EAGER grant 1548538 (JMG), NIH

250 R35GM128670 (JMG), Rudolph J. Anderson Fund Fellowship (CML), Forest B.H. and

251 Elizabeth D.W. Brown Fund Fellowship (CML and WL), NIH GM007499 (AF), The Gruber

252 Foundation (AF), and NSF GRFP DGE-1122492 (AF).

253

254

255 **Author contribution**

256 JMG and CML conceived of the project. CML, MWL, AF, AMS and WL conducted the

257 experiments and analyzed the data. JMG and CML wrote the manuscript.

258

259 **Author information**

260 **Affiliation**

261 Department of Molecular, Cellular and Developmental Biology, Yale University, New Haven,

262 CT 06511, USA

263 JMG, CML, WML, AF, AMS and WL.

264

265 **Competing interests**

266 The authors declare no competing financial interests.

267

268 **Corresponding author**

269 Dr. Joshua M. Gendron.

270

271 **Figure legends:**

272 **Figure 1. GI bridges the interactions between ZTL and UBP12 or UBP13.** (a) Yeast two-
273 hybrid showing interaction between GI and UBP12 or UBP13. The GAL4 DNA binding domain
274 (GAL4-BD) fused to UBP12 or UBP13 and either ZTL variants (ZTL and ZTL decoy), ZTL
275 targets (TOC1, PRR5 and CHE) or GI fused to GAL4 activation domain (GAL4-AD) were
276 grown on SD-LW medium for autotrophic selection and on SD-LWHA medium to test for
277 interaction. (b) Bimolecular fluorescence complementation (BiFC) assays to examine the
278 interactions of UBP12 or UBP13 and GI fused to the N- or C-terminus of Venus (YFP) were
279 performed in *Arabidopsis* protoplasts. The blue arrows indicate the interacting complex forming
280 nuclear foci. The white arrows show fluorescence signal in the cytoplasm. mCherry-VirD2NLS

281 was co-expressed as a nuclear marker, and the scale bar indicates 10 μ m. (c) The protein domains
282 of UBP12 and UBP13 required to interact with GI were tested using yeast two-hybrid assays.
283 The full-length (FL) or truncated UBP12 or UBP13 fragments as diagramed in the lower portion
284 of the panel were fused to GAL4-BD to test for interaction with GAL4-AD-GI. (d) Scatter plot
285 of proteins identified by IP-MS of ZTL decoys in the Col-0 and *gi-2* genotypes. The significance
286 of the interactions were evaluated by SAINTexpress (see Supplemental Information and Table
287 S1 for complete information) with a false discovery rate (FDR) cutoff < 0.01 and *p*-value \leq 5.37E-
288 4 to separate interacting proteins into four groups. Group I: significant interactions with ZTL
289 decoy in the *gi-2* but not Col-0. Group II: significant interactions with ZTL decoy in both Col-0
290 and *gi-2*. Group III: significant interactions with ZTL decoy in the Col-0 but not *gi-2*. Group IV:
291 Non-significant interactions with ZTL decoy in both Col-0 and *gi-2*. The interacting proteins
292 significantly enriched in the *gi-2* mutant over Col-0 were labeled along the y-axis, and the
293 proteins enriched in the Col-0 over the *gi-2* mutant were labeled along the x-axis. (e) Co-
294 immunoprecipitation assays showing that UBP12 or UBP13 interact with ZTL in a GI-dependent
295 manner. FLAG-UBP12 or FLAG-UBP13 were co-infiltrated with HA-GI and Myc-ZTL in
296 *Nicotiana benthamiana* leaves. Anti-FLAG antibody was used to immunoprecipitate FLAG-
297 UBP12 or FLAG-UBP13. Western blotting with anti-FLAG, anti-HA, or anti-Myc was used to
298 detect the presence of FLAG-UBP12, FLAG-UBP13, HA-GI, or Myc-ZTL in the
299 immunoprecipitated samples and inputs. (f) The diagram depicts the interaction between GI and
300 the MATH domain of UBP12 or UBP13, and between GI and the LOV domain of ZTL.

301

302 **Figure 2. UBP12 and UBP13 regulate the circadian clock through the same pathway as GI**
303 **and ZTL.** (a-d) The *ubp12* and *ubp13* mutants have short period phenotypes. (a, c) The periods

304 of circadian marker *pCCA1:Luciferase* (*pCCA1::LUC*) in the wildtype (Col-0) (n=20 for a and
305 n=19 for c), *ubp12-1* (n= 16), *ubp12-2w* (n= 20), *ubp13-1* (n= 15), *ubp13-2* (n= 20) and *ubp13-3*
306 (n= 14) were measured with bioluminescent assays. Each symbol represents the period from one
307 seedling, and the average period and standard deviation (SD) are labeled with gray bars. The
308 significance of period changes between wildtype and mutants were analyzed with a Welch's *t*-
309 test (***) for *p*-value < 0.001; **** for *p*-value < 0.0001). Three biological replicates were
310 performed with similar results, and one dataset is presented. (b, d) The average bioluminescence of
311 the lines displayed in a and c were plotted against time after transfer from 12h light/12h dark entrainment
312 conditions to constant light (LL). (e-f) Circadian expression of *CCA1* in Col-0, *ubp12-1*, *ubp13-1*,
313 *gi-2*, *gi-2/ubp12-1* and *gi-2/ubp13-1* after transferring to LL for 48h from the entrainment
314 conditions was measured using qRT-PCR. Subjective dark is colored with light grey. The data
315 represents the average relative expression from three biological replicates, and the error bars are
316 SD. The same Col-0 and *gi-2* data was plotted twice (in e and f) for clarity in the data
317 presentation and for comparison with the other mutant lines. (g-h) The circadian expression of
318 *CCA1* in Col-0, *ubp12-1*, *ubp13-1*, *ztl-4*, *ztl-4/ubp12-1* and *ztl-4/ubp13-1* after transferring to LL
319 for 48h from the entrainment conditions was measured using qRT-PCR. The data analyses and
320 presentation are the same as e-f. The same Col-0 and *ztl-4* data was plotted twice (in g and h). (i)
321 The circadian period of *pCCA1::LUC* in the wild type (n= 76), *ubp12-1* (n= 54), *ubp12-1* mutant
322 complemented with *pUBP12::UBP12-YFP* (n= 32) or deubiquitylating activity-dead
323 *pUBP12::UBP12CS-YFP* (n= 20). Each symbol represents the period from one seedling, and the
324 black bars indicate the average period and SD. The wild type and *ubp12-1* mutants are
325 homogenous populations, and the complementation lines are individual T1 transgenic lines. The
326 presented data is from three independent biological replicates. (j) Quantitation of the number of

327 lines, from panel i, with periods greater than the average of the *ubp12-1* mutant plus one standard
328 deviation.

329

330 **Figure 3. ZTL, GI and TOC1 protein levels are regulated by UBP12 and UBP13.** (a, c, e)

331 The protein levels of HA-tagged GI driven by native promoter (*pGI::GI-HA*), ZTL and YFP-
332 tagged TOC1 driven by the TOC1 promoter (TOC1 minigene or TMG) in the wild type (Col-0),
333 *ubp12-1* or *ubp13-1* mutants under diurnal conditions (12h light/12h dark) were detected by
334 immunoblotting. The samples from 0h to 12h after dawn were harvested in light, and the samples
335 from 16h and 20h after dawn were harvested in the dark (indicated by grey shading). The relative
336 protein levels were quantified by normalization to actin. The Col-0 or *ztl-4* samples were used as
337 negative controls for the antibodies. Plots represent the average protein levels from three
338 biological replicates, and the error bars represent standard deviation. Compared to wild type, the
339 levels of ZTL proteins in the *ubp12-1* and *ubp13-1* were below the linear range for
340 quantification. In the *ztl-4* sample, the anti-ZTL antibody recognizes a non-specific band close to
341 the size of endogenous ZTL in the long-exposure blots. (b, d, f) The relative mRNA levels of *GI-*
342 *HA*, *ZTL* or *TOC1-YFP* from the same time course samples were measured by qRT-PCR.

343

344 **Figure S1. Protein structures of UBP12 and UBP13.** UBP12 and UBP13 homologous proteins

345 contain a conserved Meprin And TRAF Homology (MATH) domain (blue) and a Ubiquitin-
346 Specific Protease (USP) domain (green) in the N-terminus. The USP has a conserved cysteine
347 protease enzymatic core (red): Cysteine Box (Cys box) and Histidine Box (His box). Mutations
348 of the conserved cysteine residue to serine in the Cys box have been shown to disrupt the

349 deubiquitylating activities of UBP12 and UBP13 (Cui et al., 2013). The numbers represent the
350 position of the amino acid sequences.

351

352 **Figure S2. Immunoprecipitation of FLAG-His-ZTL decoy in the Col-0 or *gi-2* genotypes.**

353 Immunoblots detected by anti-FLAG antibody showed that the FLAG-His-ZTL decoy and
354 FLAG-His-GFP in the Col-0 (top panel) or *gi-2* (bottom panel) can be immunoprecipitated (IP)
355 from the total protein extract (IN). The Col-0 (top) and *gi-2* (bottom) parental lines were negative
356 controls. FT: flow-through.

357

358 **Figure S3. Circadian expression of *CCA1* in the *gi-2/ubp12-2w* double mutant. Col-0, *ubp12-***

359 *2w*, *gi-2* and *gi-2/ubp12-2w* were entrained under 12h light/ 12h dark for 10d and then
360 transferred to continuous light (LL) for 48h before harvest. The expression of *CCA1* was
361 measured using qRT-PCR. The data represents the mean of the relative expression from three
362 biological replicates with the error bars showing standard deviation.

363

364 **Figure S4. The subcellular localization of UBP12 variants transiently expressed in**

365 *Nicotiana benthamiana* leaves. Leaves from 5-week-old *Nicotiana benthamiana* grown under
366 12h light/ 12h dark at 22°C were infiltrated with *Agrobacterium* expressing *pABindGFP-UBP12*
367 or *pABindGFP-UBP12C208S* with nuclear marker *pABindcherry-AS2*. The scale bar indicates
368 50µm.

369

370 **Figure S5. The proposed model for UBP12/UBP13 regulation of ZTL. (a) In the light, GI**

371 interacts with ZTL and acts as a co-chaperone, recruiting HSP90 to facilitate folding and

372 maturation of the ZTL protein. Additionally, GI physically bridges an interaction between ZTL
373 and UBP12 or UBP13. UBP12 or UBP13 stabilize the GI-ZTL protein complex before dusk. At
374 night, GI dissociates from ZTL, and ZTL mediates ubiquitylation and degradation of the TOC1
375 protein. (b) Loss of *UBP12* or *UBP13* causes instability of ZTL and GI. Interestingly, the TOC1
376 protein levels are also reduced by loss of *UBP12* or *UBP13*, mimicking the *gi* loss-of-function
377 mutant.

378

379 **Tables:**

380 **Table S1. The list of proteins identified by immunoprecipitation followed by mass**
381 **spectrometry using *35S::FLAG-His-ZTL* decoy in the Col-0 or *gi-2* background.**

382

383 **Table S2. List of primers for cloning and qRT-PCR.**

384

385 **Table S3. Results of LS Periodogram analysis of the qRT-PCR data from figure 2 e-h and**
386 **figure S3.**

387

388 **References**

- 389 **An Z, Liu Y, Ou Y, Li J, Zhang B, Sun D, Sun Y, Tang W** (2018) Regulation of the stability
390 of RGF1 receptor by the ubiquitin-specific proteases UBP12/UBP13 is critical for root
391 meristem maintenance. *Proc Natl Acad Sci U S A* **115**: 1123-1128
- 392 **Baudry A, Ito S, Song YH, Strait AA, Kiba T, Lu S, Henriques R, Pruneda-Paz JL, Chua**
393 **NH, Tobin EM, Kay SA, Imaizumi T** (2010) F-box proteins FKF1 and LKP2 act in
394 concert with ZEITLUPE to control Arabidopsis clock progression. *Plant Cell* **22**: 606-
395 622
- 396 **Carre IA** (2001) Day-length perception and the photoperiodic regulation of flowering in
397 Arabidopsis. *J Biol Rhythms* **16**: 415-423
- 398 **Cha JY, Khaleda L, Park HJ, Kim WY** (2017) A chaperone surveillance system in plant
399 circadian rhythms. *BMB Rep* **50**: 235-236

- 400 **Cha JY, Kim J, Kim TS, Zeng Q, Wang L, Lee SY, Kim WY, Somers DE** (2017)
401 GIGANTEA is a co-chaperone which facilitates maturation of ZEITLUPE in the
402 Arabidopsis circadian clock. *Nat Commun* **8**: 3
- 403 **Cui X, Lu F, Li Y, Xue Y, Kang Y, Zhang S, Qiu Q, Cui X, Zheng S, Liu B, Xu X, Cao X**
404 (2013) Ubiquitin-specific proteases UBP12 and UBP13 act in circadian clock and
405 photoperiodic flowering regulation in Arabidopsis. *Plant Physiol* **162**: 897-906
- 406 **Derkacheva M, Liu S, Figueiredo DD, Gentry M, Mozgova I, Nanni P, Tang M, Mannervik**
407 **M, Kohler C, Hennig L** (2016) H2A deubiquitinases UBP12/13 are part of the
408 Arabidopsis polycomb group protein system. *Nat Plants* **2**: 16126
- 409 **Ewan R, Pangestuti R, Thornber S, Craig A, Carr C, O'Donnell L, Zhang C, Sadanandom**
410 **A** (2011) Deubiquitinating enzymes AtUBP12 and AtUBP13 and their tobacco
411 homologue NtUBP12 are negative regulators of plant immunity. *New Phytol* **191**: 92-106
- 412 **Fujiwara S, Wang L, Han L, Suh SS, Salome PA, McClung CR, Somers DE** (2008) Post-
413 translational regulation of the Arabidopsis circadian clock through selective proteolysis
414 and phosphorylation of pseudo-response regulator proteins. *J Biol Chem* **283**: 23073-
415 23083
- 416 **Han L, Mason M, Risseuw EP, Crosby WL, Somers DE** (2004) Formation of an SCF(ZTL)
417 complex is required for proper regulation of circadian timing. *Plant J* **40**: 291-301
- 418 **Hirano A, Nakagawa T, Yoshitane H, Oyama M, Kozuka-Hata H, Lanjakornsiripan D,**
419 **Fukada Y** (2016) USP7 and TDP-43: Pleiotropic Regulation of Cryptochrome Protein
420 Stability Paces the Oscillation of the Mammalian Circadian Clock. *PLoS One* **11**:
421 e0154263
- 422 **Imaizumi T, Kay SA** (2006) Photoperiodic control of flowering: not only by coincidence.
423 *Trends Plant Sci* **11**: 550-558
- 424 **Imaizumi T, Tran HG, Swartz TE, Briggs WR, Kay SA** (2003) FKF1 is essential for
425 photoperiodic-specific light signalling in Arabidopsis. *Nature* **426**: 302-306
- 426 **Ito S, Song YH, Imaizumi T** (2012) LOV domain-containing F-box proteins: light-dependent
427 protein degradation modules in Arabidopsis. *Mol Plant* **5**: 573-582
- 428 **Jeong JS, Jung C, Seo JS, Kim JK, Chua NH** (2017) The Deubiquitinating Enzymes UBP12
429 and UBP13 Positively Regulate MYC2 Levels in Jasmonate Responses. *Plant Cell* **29**:
430 1406-1424
- 431 **Kiba T, Henriques R, Sakakibara H, Chua NH** (2007) Targeted degradation of PSEUDO-
432 RESPONSE REGULATOR5 by an SCFZTL complex regulates clock function and
433 photomorphogenesis in Arabidopsis thaliana. *Plant Cell* **19**: 2516-2530
- 434 **Kim J, Geng R, Gallenstein RA, Somers DE** (2013) The F-box protein ZEITLUPE controls
435 stability and nucleocytoplasmic partitioning of GIGANTEA. *Development* **140**: 4060-
436 4069
- 437 **Kim TS, Kim WY, Fujiwara S, Kim J, Cha JY, Park JH, Lee SY, Somers DE** (2011) HSP90
438 functions in the circadian clock through stabilization of the client F-box protein
439 ZEITLUPE. *Proc Natl Acad Sci U S A* **108**: 16843-16848
- 440 **Kim WY, Fujiwara S, Suh SS, Kim J, Kim Y, Han L, David K, Putterill J, Nam HG,**
441 **Somers DE** (2007) ZEITLUPE is a circadian photoreceptor stabilized by GIGANTEA in
442 blue light. *Nature* **449**: 356-360
- 443 **Kim WY, Geng R, Somers DE** (2003) Circadian phase-specific degradation of the F-box
444 protein ZTL is mediated by the proteasome. *Proc Natl Acad Sci U S A* **100**: 4933-4938

- 445 **Kim Y, Lim J, Yeom M, Kim H, Kim J, Wang L, Kim WY, Somers DE, Nam HG** (2013)
446 ELF4 regulates GIGANTEA chromatin access through subnuclear sequestration. *Cell*
447 *Rep* **3**: 671-677
- 448 **Komander D, Clague MJ, Urbe S** (2009) Breaking the chains: structure and function of the
449 deubiquitinases. *Nat Rev Mol Cell Biol* **10**: 550-563
- 450 **Krahmer J, Goralogia GS, Kubota A, Zardilis A, Johnson RS, Song YH, MacCoss MJ, Le**
451 **Bihan T, Halliday KJ, Imaizumi T, Millar AJ** (2019) Time-resolved interaction
452 proteomics of the GIGANTEA protein under diurnal cycles in Arabidopsis. *FEBS Lett*
453 **593**: 319-338
- 454 **Lee C-M, Feke A, Li M-W, Adamchek C, Webb K, Pruneda-Paz J, Bennett EJ, Kay SA,**
455 **Gendron JM** (2018) Decoys untangle complicated redundancy and reveal targets of
456 circadian clock F-box proteins. *Plant Physiology* **177**:1170-1186
- 457 **Luo W, Li Y, Tang CH, Abruzzi KC, Rodriguez J, Pescatore S, Rosbash M** (2012) CLOCK
458 deubiquitylation by USP8 inhibits CLK/CYC transcription in *Drosophila*. *Genes Dev* **26**:
459 2536-2549
- 460 **Mas P, Kim WY, Somers DE, Kay SA** (2003) Targeted degradation of TOC1 by ZTL
461 modulates circadian function in *Arabidopsis thaliana*. *Nature* **426**: 567-570
- 462 **Mevissen TET, Komander D** (2017) Mechanisms of Deubiquitinase Specificity and
463 Regulation. *Annu Rev Biochem* **86**: 159-192
- 464 **Mizoguchi T, Yoshida R** (2009) Punctual coordination: switching on and off for flowering
465 during a day. *Plant Signal Behav* **4**: 113-115
- 466 **Nozue K, Covington MF, Duek PD, Lorrain S, Fankhauser C, Harmer SL, Maloof JN**
467 (2007) Rhythmic growth explained by coincidence between internal and external cues.
468 *Nature* **448**: 358-361
- 469 **Papp SJ, Huber AL, Jordan SD, Kriebs A, Nguyen M, Moresco JJ, Yates JR, Lamia KA**
470 (2015) DNA damage shifts circadian clock time via Hausp-dependent Cry1 stabilization.
471 *Elife* **4**
- 472 **Pudasaini A, Shim JS, Song YH, Shi H, Kiba T, Somers DE, Imaizumi T, Zoltowski BD**
473 (2017) Kinetics of the LOV domain of ZEITLUPE determine its circadian function in
474 *Arabidopsis*. *Elife* **6**
- 475 **Pudasaini A, Zoltowski BD** (2013) Zeitlupe senses blue-light fluence to mediate circadian
476 timing in *Arabidopsis thaliana*. *Biochemistry* **52**: 7150-7158
- 477 **Salome PA, McClung CR** (2004) The *Arabidopsis thaliana* clock. *J Biol Rhythms* **19**: 425-435
- 478 **Scoma HD, Humby M, Yadav G, Zhang Q, Fogerty J, Besharse JC** (2011) The de-
479 ubiquitylating enzyme, USP2, is associated with the circadian clockwork and regulates
480 its sensitivity to light. *PLoS One* **6**: e25382
- 481 **Somers DE, Kim WY, Geng R** (2004) The F-box protein ZEITLUPE confers dosage-dependent
482 control on the circadian clock, photomorphogenesis, and flowering time. *Plant Cell* **16**:
483 769-782
- 484 **Somers DE, Schultz TF, Milnamow M, Kay SA** (2000) ZEITLUPE encodes a novel clock-
485 associated PAS protein from *Arabidopsis*. *Cell* **101**: 319-329
- 486 **Takase T, Nishiyama Y, Tanihigashi H, Ogura Y, Miyazaki Y, Yamada Y, Kiyosue T**
487 (2011) LOV KELCH PROTEIN2 and ZEITLUPE repress *Arabidopsis* photoperiodic
488 flowering under non-inductive conditions, dependent on FLAVIN-BINDING KELCH
489 REPEAT F-BOX1. *Plant J* **67**: 608-621

- 490 **Yang Y, Duguay D, Bedard N, Rachalski A, Baquiran G, Na CH, Fahrenkrug J, Storch**
491 **KF, Peng J, Wing SS, Cermakian N** (2012) Regulation of behavioral circadian rhythms
492 and clock protein PER1 by the deubiquitinating enzyme USP2. *Biol Open* **1**: 789-801
493 **Yanovsky MJ, Kay SA** (2002) Molecular basis of seasonal time measurement in *Arabidopsis*.
494 *Nature* **419**: 308-312
495 **Zhou H, Zhao J, Cai J, Patil SB** (2017) UBIQUITIN-SPECIFIC PROTEASES function in
496 plant development and stress responses. *Plant Mol Biol* **94**: 565-576
497 **Zielinski T, Moore AM, Troup E, Halliday KJ, Millar AJ** (2014) Strengths and limitations of
498 period estimation methods for circadian data. *PLoS One* **9**: e96462
499

Supplemental Information

Materials and Methods

Plant materials and growth conditions

The *Arabidopsis* seeds of Col-0, *ubp12-1* (CS423387), *ubp12-2w* (CS2103163), *ubp13-1* (SALK_128312), *ubp13-2* (SALK_024054), *ubp13-3* (SALK_132368)¹, *gi-2* (cs3370)^{2,3}, *ztl-4* (SALK_012440)⁴, *pGI::GI-HA* (CS66130)⁵ and TMG (CS31390)⁶ were described previously and obtained from ABRC. The *ubp12-1/gi-2*, *ubp12-2w/gi-2*, *ubp13-1/gi-2*, *ubp12-1/ztl-4* and *ubp13-1/ztl-4* double mutants were generated by crossing and genotyped by PCR. The *pGI::GI-HA* and TMG lines were crossed to *ubp12-1* and *ubp13-1*, and the homozygous lines were selected by genotyping and gentamycin resistance.

For IP-MS, the *35S::FLAG-His-ZTL-decoy* transgenic lines and *35S::FLAG-His-GFP* control were described previously⁷, and the same constructs were transformed into the *gi-2* background by floral-dip method⁸.

For the bioluminescent assays, the circadian reporter line *pCCA1::Luciferase* (*pCCA1::LUC*)⁹ was crossed to the *ubp12* and *ubp13* mutants. The *pUBP12::UBP12-YFP* variants (see Cloning section) were transformed into *pCCA1::LUC/ubp12-1* by floral-dip⁸ for complementation experiments.

For growth conditions of *Arabidopsis* seedlings, the seeds were surface sterilized with ethanol, cold stratified, plated on ½ strength MS (Murashige and Skoog medium, Caisson Laboratories, MSP01) medium with 0.8% Agar (AmericanBio, AB01185), and grown at 22°C under 12h light/12h dark as described previously⁷ unless specified otherwise. For soil-grown conditions, plants were grown in Fafard-2 mix under 16h light/8h dark at 22 °C.

For circadian experiments, seedlings were grown on ½ strength MS medium under 12h light/12h dark at 22 °C for 10d, transferred to continuous light (LL) at 22 °C for 48h before starting harvest. For the 12h light/12 dark (LD) experiments, 12-day-old seedlings grown on ½ strength MS medium were used.

Cloning

The GATEWAY pENTR™/D-TOPO entry vectors (Thermo Fisher Scientific, K240020) of ZTL full-length, ZTL decoy, CHE, TOC1 and PRR5 were obtained from previous reports^{7,9,10}. For GI, UB12 and UB13, the full-length coding regions were amplified from cDNA by PCR and cloned into pENTR™/D-TOPO vectors. These entry clones were then sub-cloned into GATEWAY compatible yeast two-hybrid vectors (pGADT7-GW and pGBKT7-GW)¹¹ or BiFC vectors (pUC-DEST-VYCE®GW and pUC-DEST-VYNE®GW)¹² with GATEWAY recombination cloning (Thermo Fisher Scientific).

To construct the fragments of UB12 and UB13 into yeast two-hybrid pGADT7-GW vectors, the desired fragments were first amplified from the full-length UB12 or UB13 entry vectors by PCR and cloned into pENTR™/D-TOPO vectors before being sub-cloned into pGADT7-GW with GATEWAY cloning.

For the UBP12 complementation plasmids, the pENTRTM/D-TOPO-UBP12-NS vector served as template for site-directed mutagenesis to introduce a Cys to Ser mutation at a.a. 208 position using Q5® Site-Directed Mutagenesis Kit (NEB, E0554). Subsequently, UBP12-NS and UBP12C208S-NS in the pENTRTM/D-TOPO entry vectors were sub-cloned into a modified GATEWAY compatible pGreenBarT vector¹² with 1.7k bp upstream of ATG of *UBP12* promoter region in the KpnI/XhoI sites. The primers used for cloning were listed in Table S2.

Yeast two-hybrid

ZTL, ZTL decoy, GI, TOC1, PRR5 and CHE were fused to the GAL4-BD in pGBKT7-GW vectors, and the full-length or fragments of UBP12 and UBP13 were fused to the GAL4-AD in pGADT7-GW vectors by GATEWAY cloning. The interactions were tested on synthetic dropout medium as described previously⁷.

Bimolecular fluorescence complementation (BiFC) and confocal microscopy

The coding region of GI, UBP12 or UBP13 in the GATEWAY entry vectors were cloned into protoplast GATEWAY destination vectors pUC-DEST-VYCE®GW and pUC-DEST-VYNE(R)GW¹² respectively for transient transfections into protoplasts. *pSAT6-mCherry-VirD2NLS* was used as a nuclear marker. The protoplasts were isolated from 3- to 4-week-old *Arabidopsis* (Col-0) grown at 22°C under 8h light/16h dark and transfected following the protocol of tape-*Arabidopsis* sandwich method¹³. After 14-18 h incubation in low-light conditions, protoplasts were imaged on a Nikon Ti microscope with using a 60X 1.4 NA plan Apo objective lens as described previously¹⁴. The images were analyzed with FIJI¹⁵.

Immunoprecipitation and mass spectrometry (IP-MS)

For the ZTL decoys in Col-0 background, homozygous *35S::FLAG-His-ZTL-decoy* transgenic lines along with Col-0 and *35S::FLAG-His-GFP* controls were used. For the ZTL decoys in the *gi-2* background, three independent T2 transgenic lines of *35S::FLAG-His-ZTL-decoy/gi-2* and *35S::FLAG-His-GFP/gi-2* were selected on ½ strength MS plates with 15 µg/ml ammonium glufosinate before being transferred to soil. Twenty-one-day-old soil-grown plants were entrained in 12 h light/12 h dark at 22°C for 7 days prior to harvest. Leaf tissues were collected at 9 h after dawn for subsequent IP-MS. One-step IP-MS and MS spectral analyses were carried out as documented⁷ with minor changes. The MS/MS spectral were searched against the SwissProt_2017 tax: *Arabidopsis thaliana* (thale cress) database (February 2017) using MASCOT MS/MS ion search engine version 2.6.0¹⁶ with the following parameters: up to 2 missed cleavages; variable modifications included Acetyl (K), GlyGly(K), Oxidation (M), Phospho (ST), Phospho (Y); peptide tolerance ± 10 ppm; MS/MS tolerance ± 5 Da; peptide charge 2+ and 3+. The protein lists identified by MASCOT were first filtered out non-specific interactions by removing proteins only present in the controls (Col-0, *gi-2*, *35S::FLAG-His-GFP/Col-0* and *35S::FLAG-His-GFP/gi-2*). The SAINTexpress algorithm^{17,18} were further performed to determine the significance of protein-protein interactions.

Bioluminescent assays

The *Arabidopsis* seedlings bearing *pCCA1::LUC* in the wild type (Col-0), *ubp12* or *ubp13* mutants were grown in ½ strength MS medium and entrained in 12h light/12h dark for 7 days prior to being transferred to new ½ strength MS plates and constant light (LL) for circadian free-run experiments. For the various *pUBP12::UBP12-YFP* complementation T1 lines in the *pCCA1::LUC/ubp12-1* background, seedlings were first screened and entrained on the ½ strength MS plates containing 7.5 µg/ml ammonium glufosinate prior to being transferred to ½ strength MS medium and LL. The measurement of luciferase activities and analyses were described as previously⁷.

Real-Time Quantitative Reverse Transcription PCR (qRT-PCR)

RNA extraction, reverse-transcription and constitution of qPCR reactions were followed as described previously⁷, except for minor modifications. Four hundred ng total RNA were used for reverse transcription reactions. For semi-quantification of gene expression, *IPP2* (AT3G02780) was used as an internal control. The relative expression represents means of $2^{-(\Delta CT)}$ from three biological replicates, in which $\Delta CT = (CT \text{ of Gene of Interest} - CT \text{ of } IPP2)$. The primers were listed in Table S2.

Immunoblotting

The procedure of protein extraction from *Arabidopsis* seedlings, separation, detection with antibodies and quantification are described as previously⁷, except 60µg total protein were used for immunoblotting. The primary antibodies used for detection are: for GI-HA, anti-HA-Biotin antibody (1:1000, 12158167001, Millipore-Sigma); for ZTL, anti-ZTL antibody¹⁹ (1:200); for TMG, anti-GFP (1:10000, ab-290, Abcam); for FLAG-ZTL decoy, anti-FLAG antibody (1:1000, F7425, Millipore-Sigma). To quantify expression levels, the levels of target proteins were normalized to actin (anti-Actin antibody, 1:2000, SAB4301137, Millipore-Sigma).

Transient expression in *Nicotiana benthamiana* and confocal microscopy

UBP12-NS and, UBP12C208S-NS in the pENTRTM/D-TOPO vectors were subcloned into inducible GATEWAY destination pABindGFP vectors²⁰ and transformed into the *Agrobacterium tumefaciens* strain *GV3101* for transient expression in *Nicotiana benthamiana*. The *Agrobacterium* culture of pABindGFP-UBP12 or pABindGFP-UBP12C208S and the nuclear marker pABindcherry-AS2²¹ were pelleted and resuspended in the infiltration solution (5% (w/v) Sucrose, 450 µM acetosyringone and 0.01% (v/v) Silwet). The bacterial infiltration solution was incubated at 4°C for 2h before infiltrated into 5-week-old *Nicotiana benthamiana* leaves. After 20h of infiltration, the protein expression was induced by spaying leaves with 20 µM β-estradiol in 0.1% Tween 20. The leaves were imaged after 18h of induction.

The leaf samples were imaged on a Zeiss LSM510 confocal microscope with a Plan-Apochromat 40x/1.3 Oil objective. GFP was excited using 488 nm Argon laser and observed through a

505/530 nm bandpass filter. mCherry was excited using 543 nm HeNe laser and observed through a 585/615 nm bandpass filter. The images were processed with FIJI¹⁵.

Co-immunoprecipitation (co-IP) using *Nicotiana benthamiana* transient expression system

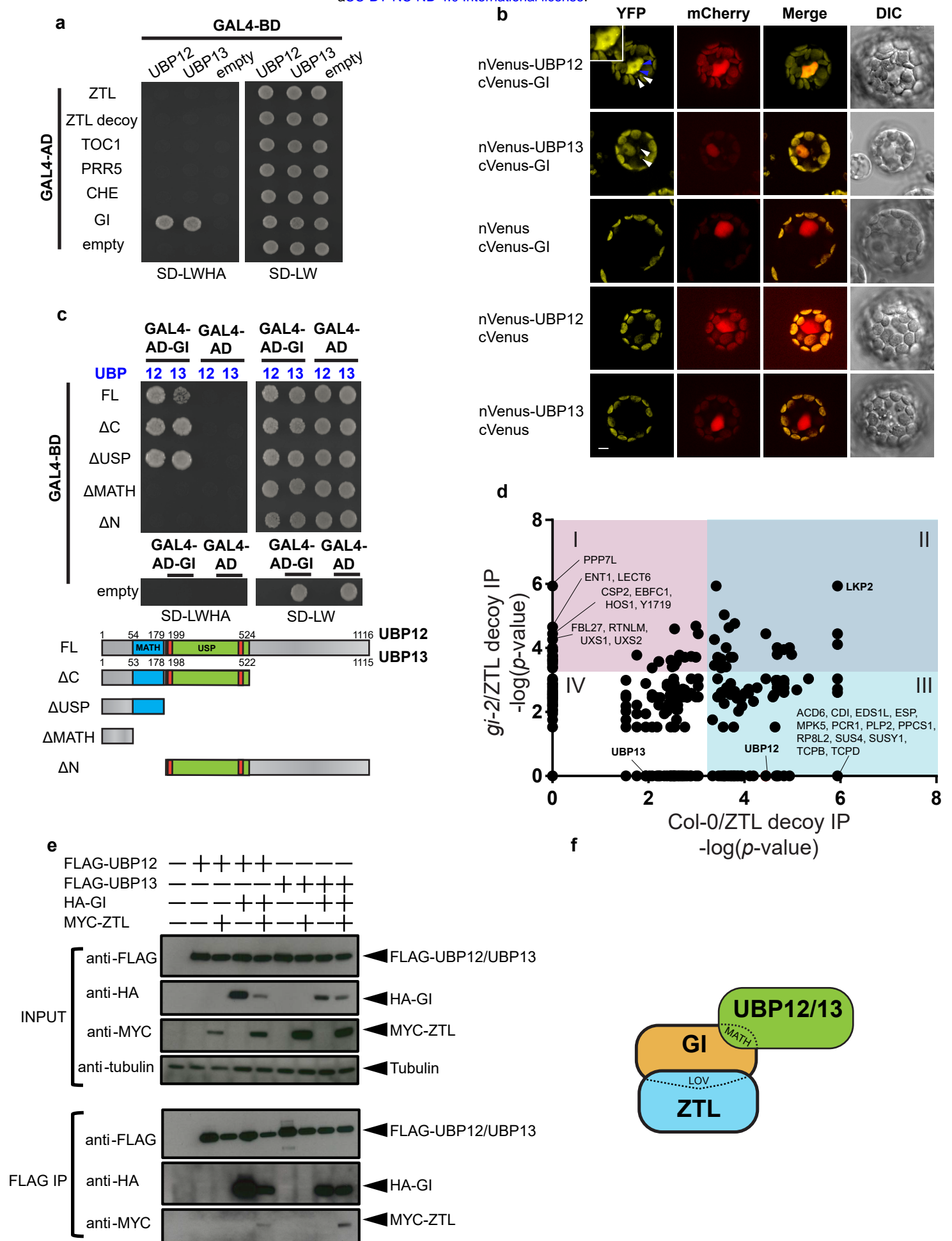
The full-length coding sequences of ZTL, GI, UBP12 and UBP13 in the pENTR™/D-TOPO vectors were subcloned into pEarlygate203, pEarlygate201 and pEarlygate202 plant binary vectors²² respectively and transformed into *Agrobacterium tumefaciens* strain *GV3101*. Agro-infiltration into *Nicotiana benthamiana* leaves was described in the previous section. In this co-immunoprecipitation experiment co-infiltration with P19 in the EHA105 *Agrobacterium* strain was used to increase expression of the transgenes. The leaf samples were harvested after 48h of infiltration and snap frozen with liquid nitrogen. Protein extraction and co-immunoprecipitation with Anti-FLAG® M2 Magnetic Beads (M8823, Millipore-Sigma), and a one-step IP protocol was used as described previously^{7,23}. The inputs and IP samples were resolved on NuPAGE 4-12% Bis-Tris Protein Gels (NP0321, Thermo Fisher Scientific) for immunoblotting. The primary antibodies used for detection are: for MYC-ZTL, anti-MYC antibody (1:10000, C3956, Millipore-Sigma); for HA-GI, anti-HA antibody (1:5000, H3663, Millipore-Sigma); for FLAG-UBP12 and FLAG-UBP13, anti-FLAG antibody (1:5000, F1804, Millipore-Sigma); for loading control, anti-tubulin antibody (1:5000, T5168, Millipore-Sigma).

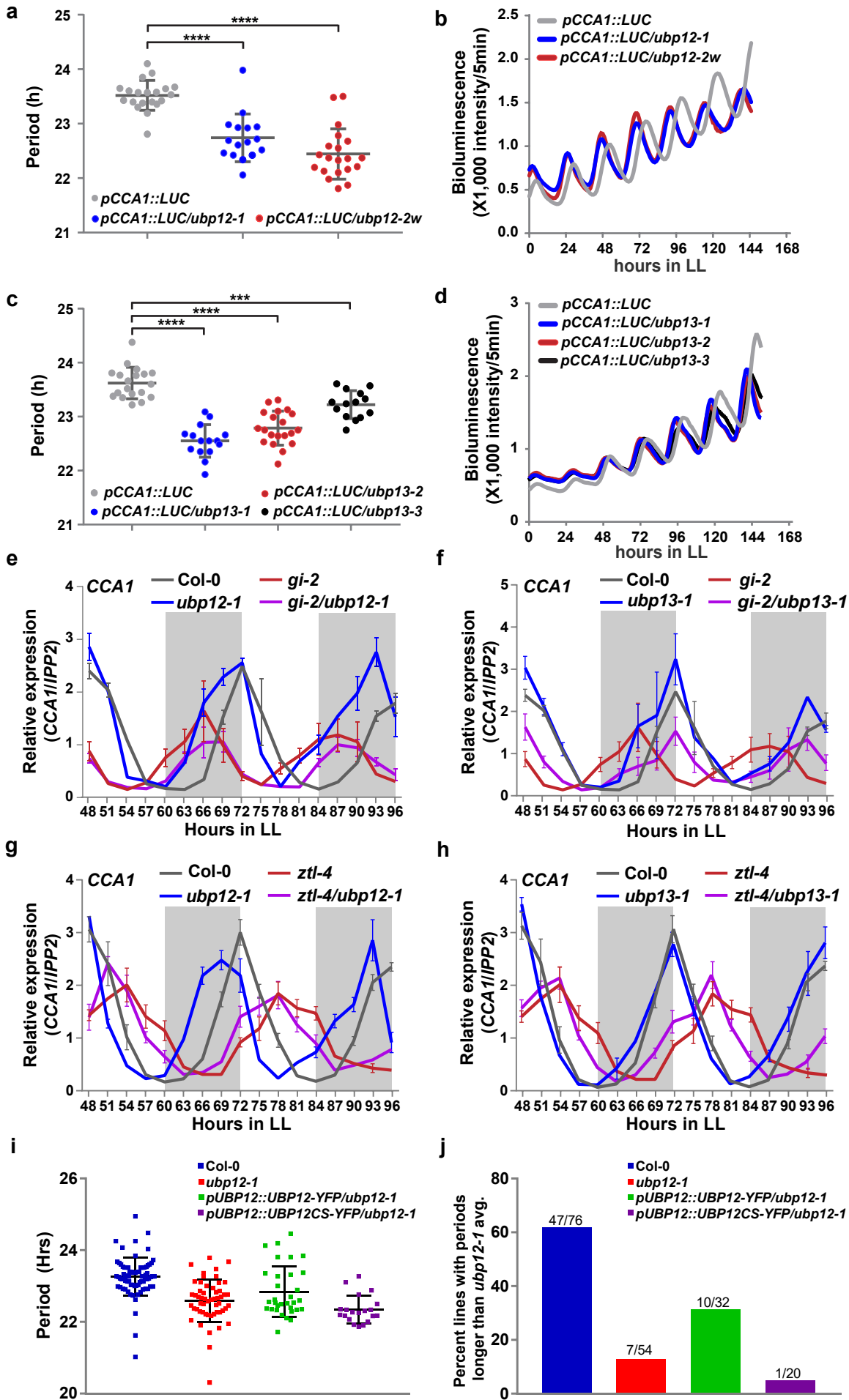
Data Availability

The raw data of mass spectrometry experiments will be deposited to PRIDE (<https://www.ebi.ac.uk/pride/archive/>).

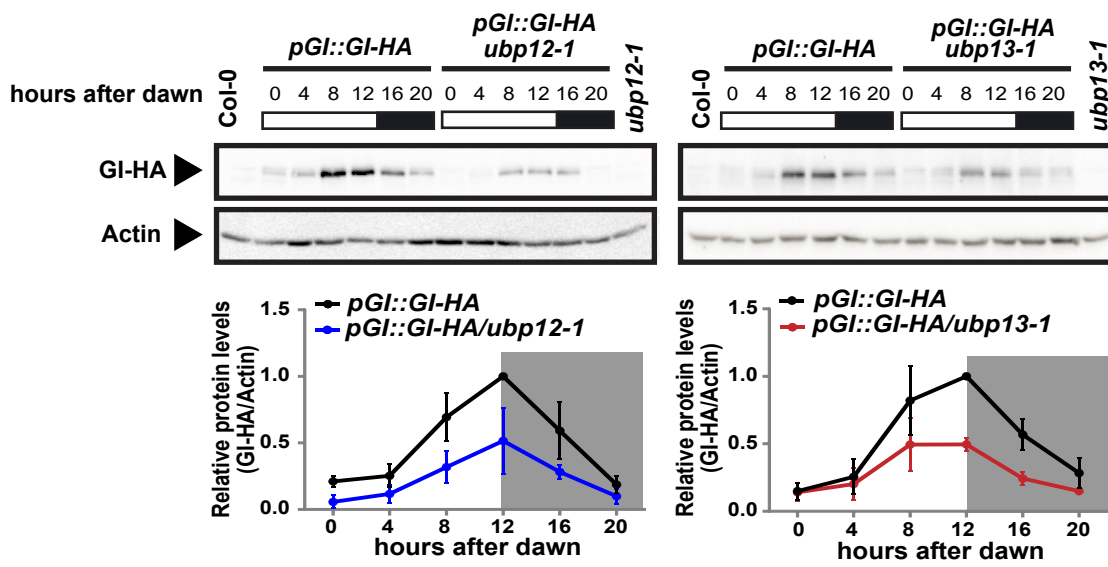
- 1 Cui, X. *et al.* Ubiquitin-specific proteases UBP12 and UBP13 act in circadian clock and photoperiodic flowering regulation in Arabidopsis. *Plant Physiol* **162**, 897-906, doi:10.1104/pp.112.213009 (2013).
- 2 Hirono, Y. & Redei, G. P. Induced Premeiotic Exchange of Linked Markers in the Angiosperm Arabidopsis. *Genetics* **51**, 519-526 (1965).
- 3 Koornneef, M., Hanhart, C. J. & van der Veen, J. H. A genetic and physiological analysis of late flowering mutants in Arabidopsis thaliana. *Mol Gen Genet* **229**, 57-66 (1991).
- 4 Salome, P. A. & McClung, C. R. PSEUDO-RESPONSE REGULATOR 7 and 9 are partially redundant genes essential for the temperature responsiveness of the Arabidopsis circadian clock. *Plant Cell* **17**, 791-803, doi:10.1105/tpc.104.029504 (2005).
- 5 David, K. M., Armbruster, U., Tama, N. & Putterill, J. Arabidopsis GIGANTEA protein is post-transcriptionally regulated by light and dark. *FEBS Lett* **580**, 1193-1197, doi:10.1016/j.febslet.2006.01.016 (2006).
- 6 Mas, P., Kim, W. Y., Somers, D. E. & Kay, S. A. Targeted degradation of TOC1 by ZTL modulates circadian function in Arabidopsis thaliana. *Nature* **426**, 567-570, doi:10.1038/nature02163 (2003).
- 7 Lee, C. M. *et al.* Decoys Untangle Complicated Redundancy and Reveal Targets of Circadian Clock F-Box Proteins. *Plant physiology* **177**, 1170-1186, doi:10.1104/pp.18.00331 (2018).

- 8 Clough, S. J. & Bent, A. F. Floral dip: a simplified method for *Agrobacterium*-mediated transformation of *Arabidopsis thaliana*. *Plant J* **16**, 735-743 (1998).
- 9 Pruneda-Paz, J. L., Breton, G., Para, A. & Kay, S. A. A functional genomics approach reveals CHE as a component of the *Arabidopsis* circadian clock. *Science* **323**, 1481-1485, doi:10.1126/science.1167206 (2009).
- 10 Nakamichi, N. *et al.* PSEUDO-RESPONSE REGULATORS 9, 7, and 5 are transcriptional repressors in the *Arabidopsis* circadian clock. *Plant Cell* **22**, 594-605, doi:10.1105/tpc.109.072892 (2010).
- 11 Lu, Q. *et al.* *Arabidopsis* homolog of the yeast TREX-2 mRNA export complex: components and anchoring nucleoporin. *Plant J* **61**, 259-270, doi:10.1111/j.1365-313X.2009.04048.x (2010).
- 12 Wu, S. *et al.* A plausible mechanism, based upon Short-Root movement, for regulating the number of cortex cell layers in roots. *Proc Natl Acad Sci U S A* **111**, 16184-16189, doi:10.1073/pnas.1407371111 (2014).
- 13 Wu, F. H. *et al.* Tape-*Arabidopsis* Sandwich - a simpler *Arabidopsis* protoplast isolation method. *Plant Methods* **5**, 16, doi:10.1186/1746-4811-5-16 (2009).
- 14 Penfield, L. *et al.* Dynein-pulling forces counteract lamin-mediated nuclear stability during nuclear envelope repair. *Mol Biol Cell*, doi:10.1091/mbc.E17-06-0374 (2018).
- 15 Schindelin, J. *et al.* Fiji: an open-source platform for biological-image analysis. *Nat Methods* **9**, 676-682, doi:10.1038/nmeth.2019 (2012).
- 16 Perkins, D. N., Pappin, D. J., Creasy, D. M. & Cottrell, J. S. Probability-based protein identification by searching sequence databases using mass spectrometry data. *Electrophoresis* **20**, 3551-3567, doi:10.1002/(SICI)1522-2683(19991201)20:18<3551::AID-ELPS3551>3.0.CO;2-2 (1999).
- 17 Teo, G. *et al.* SAINTexpress: improvements and additional features in Significance Analysis of INTeractome software. *J Proteomics* **100**, 37-43, doi:10.1016/j.jprot.2013.10.023 (2014).
- 18 Goldfarb, D., Hast, B. E., Wang, W. & Major, M. B. Spotlight: web application and augmented algorithms for predicting co-complexed proteins from affinity purification--mass spectrometry data. *J Proteome Res* **13**, 5944-5955, doi:10.1021/pr5008416 (2014).
- 19 Kim, W. Y., Geng, R. & Somers, D. E. Circadian phase-specific degradation of the F-box protein ZTL is mediated by the proteasome. *Proc Natl Acad Sci U S A* **100**, 4933-4938, doi:10.1073/pnas.0736949100 (2003).
- 20 Bleckmann, A., Weidtkamp-Peters, S., Seidel, C. A. & Simon, R. Stem cell signaling in *Arabidopsis* requires CRN to localize CLV2 to the plasma membrane. *Plant Physiol* **152**, 166-176, doi:10.1104/pp.109.149930 (2010).
- 21 Rast, M. I. & Simon, R. *Arabidopsis* JAGGED LATERAL ORGANS acts with ASYMMETRIC LEAVES2 to coordinate KNOX and PIN expression in shoot and root meristems. *Plant Cell* **24**, 2917-2933, doi:10.1105/tpc.112.099978 (2012).
- 22 Earley, K. W. *et al.* Gateway-compatible vectors for plant functional genomics and proteomics. *Plant J* **45**, 616-629, doi:10.1111/j.1365-313X.2005.02617.x (2006).
- 23 Lee, C. M., Adamchek, C., Feke, A., Nusinow, D. A. & Gendron, J. M. Mapping Protein-Protein Interactions Using Affinity Purification and Mass Spectrometry. *Methods in molecular biology (Clifton, N.J.)* **1610**, 231-249, doi:10.1007/978-1-4939-7003-2_15 (2017).

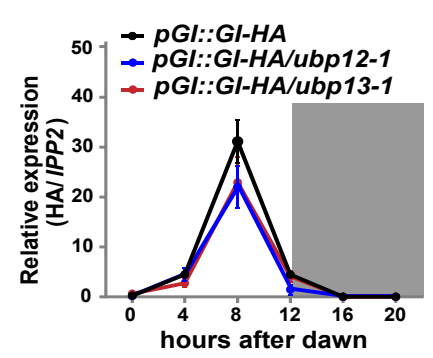




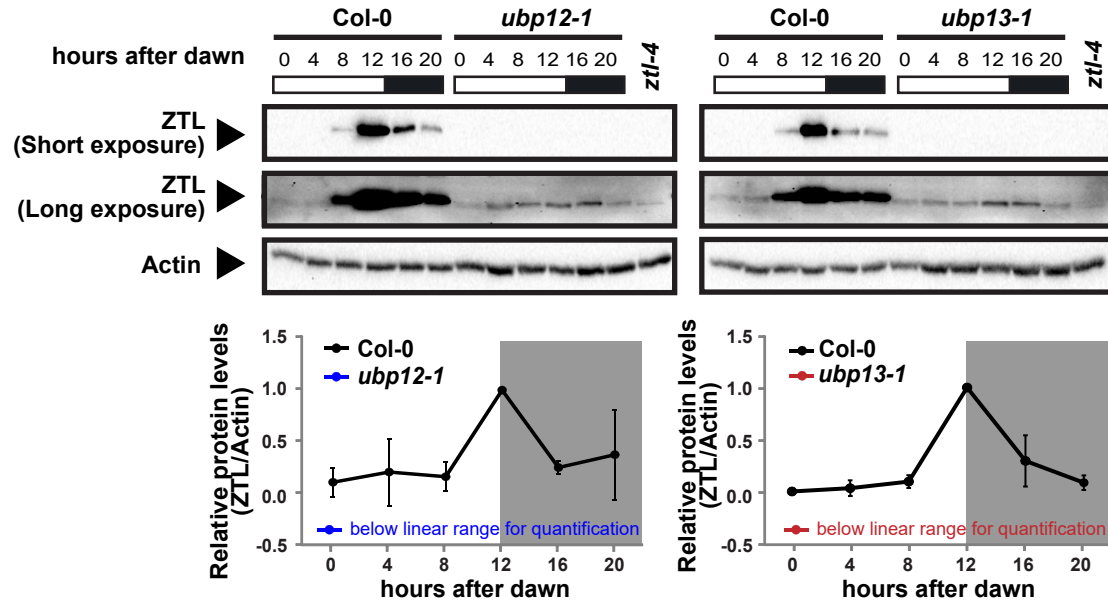
a



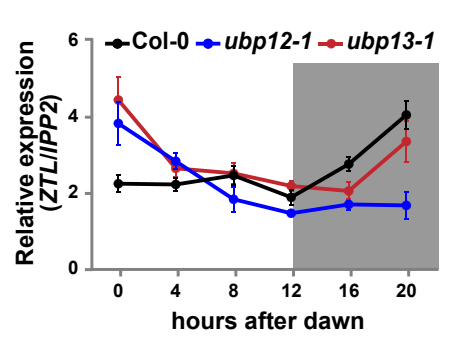
b



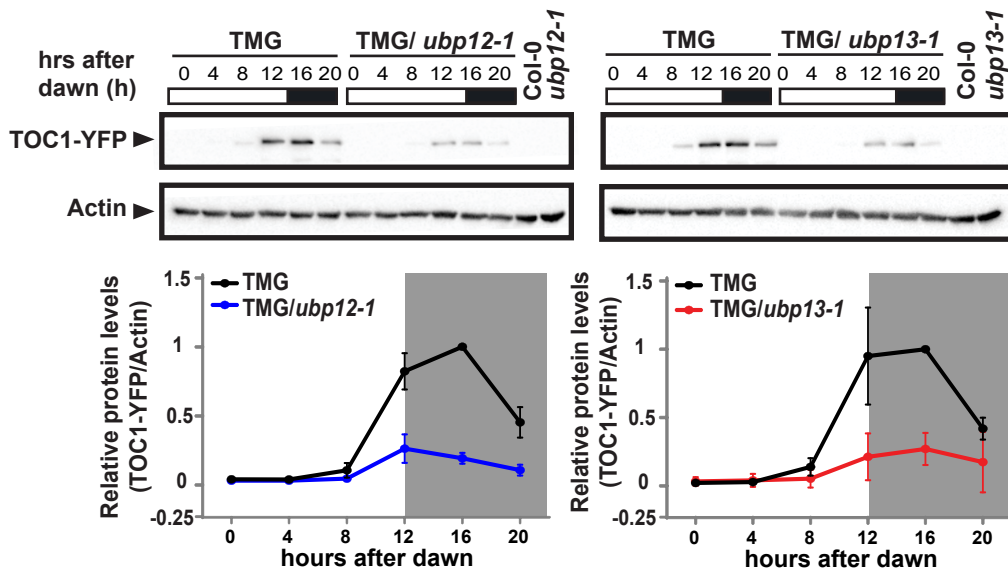
c



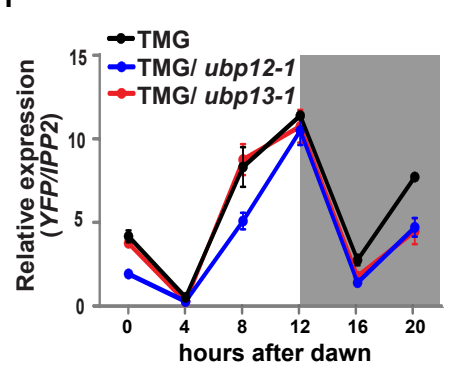
d

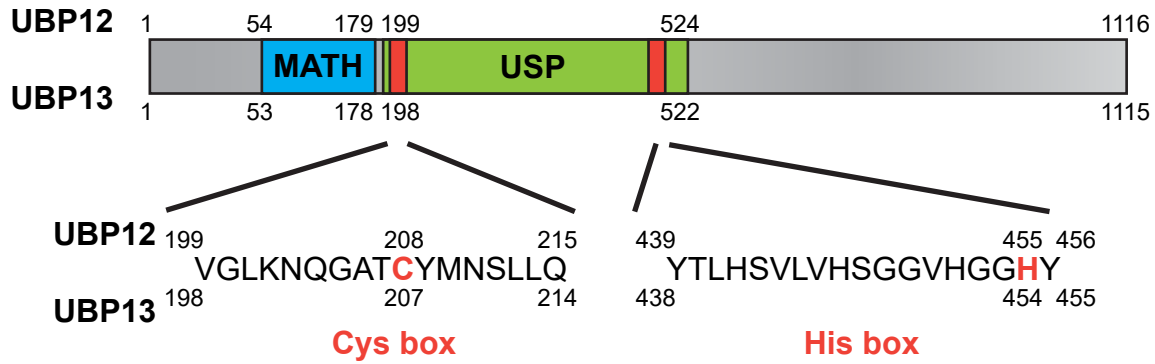


e

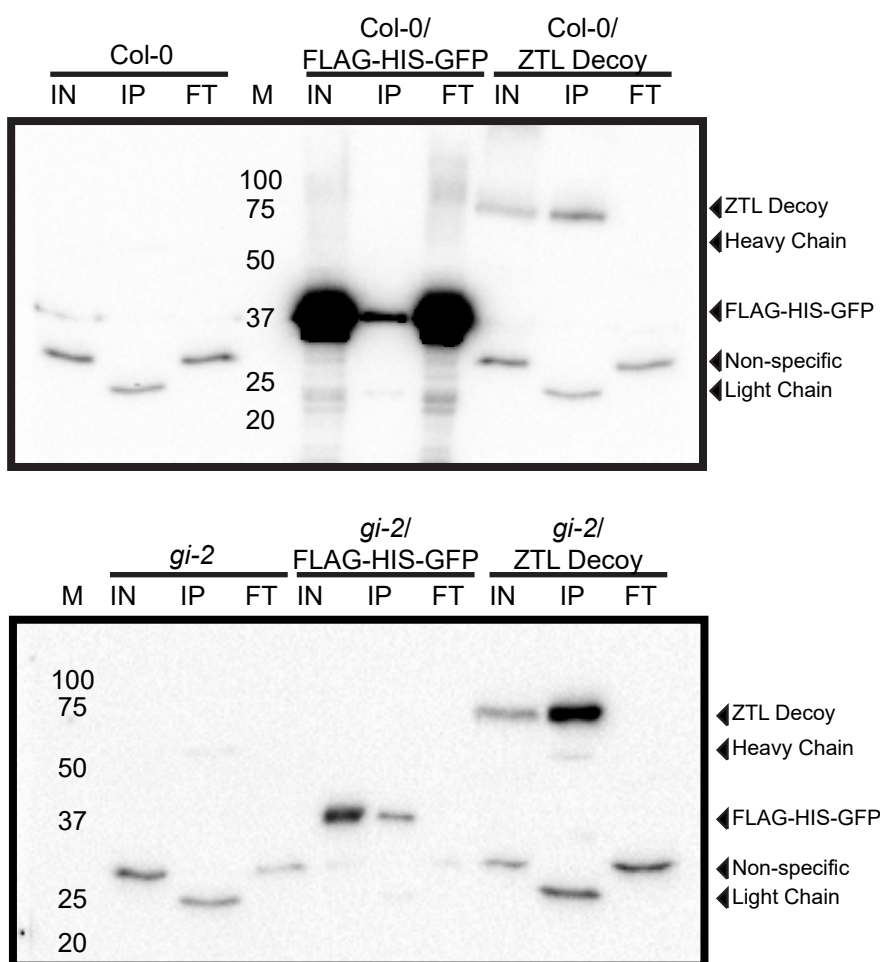


f

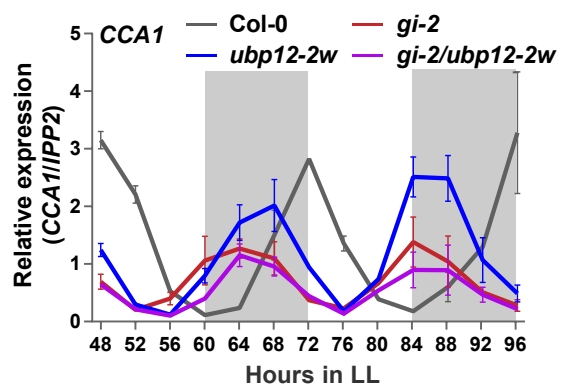




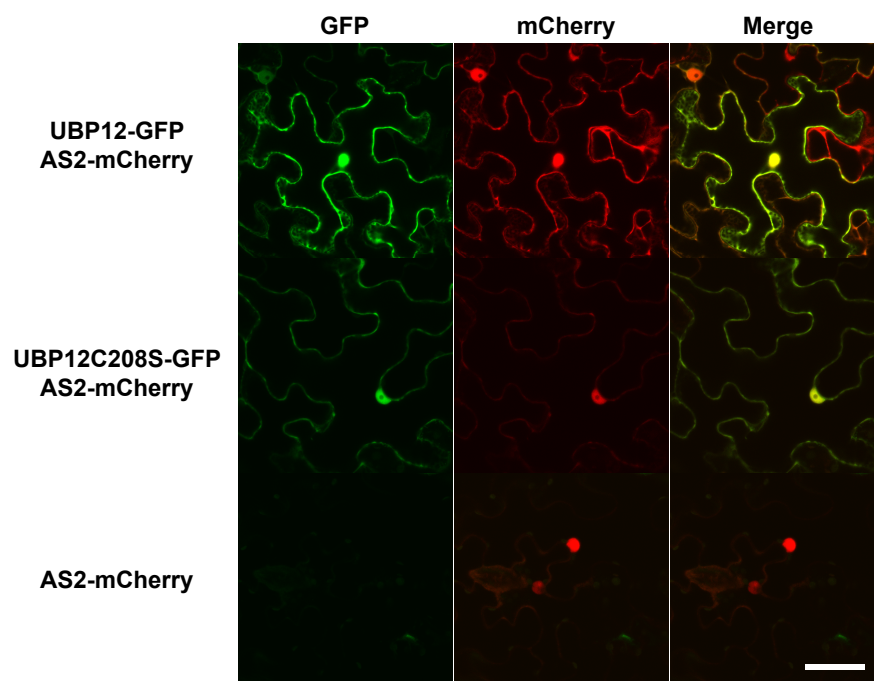
Lee *et al.* Figure S2



Lee *et al.* Figure S3



Lee *et al.* Figure S4



Lee *et al.* Figure S5

